

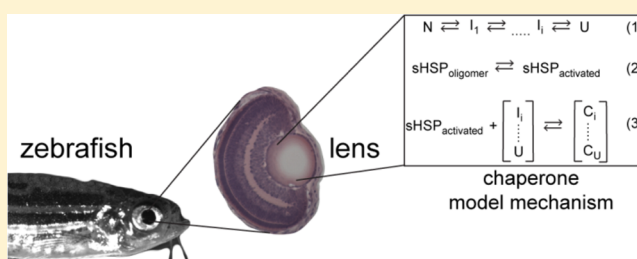
Species-Specific Structural and Functional Divergence of α -Crystallins: Zebrafish α Ba- and Rodent α A^{ins}-Crystallin Encode Activated Chaperones

Hanane A. Koteiche,[‡] Derek P. Claxton,[‡] Sanjay Mishra, Richard A. Stein, Ezelle T. McDonald, and Hassane S. Mchaourab*

Department of Molecular Physiology and Biophysics, Vanderbilt University School of Medicine, Nashville, Tennessee 37232, United States

S Supporting Information

ABSTRACT: In addition to contributing to lens optical properties, the α -crystallins are small heat shock proteins that possess chaperone activity and are predicted to bind and sequester destabilized proteins to delay cataract formation. The current model of α -crystallin chaperone mechanism envisions a transition from the native oligomer to an activated form that has higher affinity to non-native states of the substrate. Previous studies have suggested that this oligomeric plasticity is encoded in the primary sequence and controls access to high affinity binding sites within the N-terminal domain. Here, we further examined the role of sequence variation in the context of species-specific α -crystallins from rat and zebrafish. Alternative splicing of the α A gene in rodents produces α A^{ins}, which is distinguished by a longer N-terminal domain. The zebrafish genome includes duplicate α B-crystallin genes, α Ba and α Bb, which display divergent primary sequence and tissue expression patterns. Equilibrium binding experiments were employed to quantitatively define chaperone interactions with a destabilized model substrate, T4 lysozyme. In combination with multiangle light scattering, we show that rat α A^{ins} and zebrafish α -crystallins display distinct global structural properties and chaperone activities. Notably, we find that α A^{ins} and α Ba demonstrate substantially enhanced chaperone function relative to other α -crystallins, binding the same substrate more than 2 orders of magnitude higher affinity and mimicking the activity of fully activated mammalian small heat shock proteins. These results emphasize the role of sequence divergence as an evolutionary strategy to tune chaperone function to the requirements of the tissues and organisms in which they are expressed.



As a consequence of terminal differentiation, the organelle-free fiber cells of the ocular lens are presented with the challenge of producing an appropriate refractive medium and maintaining optical clarity for a lifetime. Expression of the crystallins, which possess uniquely high solubility and stability, addresses both issues at two fundamental levels. Serving as principle units of supramolecular structure, the crystallins are primary to lens transparency and refractivity through finely tuned protein–protein interactions that achieve the short-range order required to focus light onto the retina.^{2–5} In addition, the α -crystallins, composed of distinct α A and α B polypeptide chains, share sequence similarity to small heat shock proteins^{6,7} (sHSP) and demonstrate characteristics of molecular chaperones *in vitro*.⁸

Accumulation of age-related posttranslational modifications^{9–12} to lens proteins reduces thermodynamic stability (ΔG_{unf}) and shifts the folding equilibrium toward non-native states. In the absence of protein turnover, the increasing prevalence of non-native states in the dense protein milieu drives hydrophobic associations.^{13,14} As a chaperone, α -crystallin is postulated to bind destabilized proteins that would otherwise form insoluble aggregates potentially leading

to opacification.^{15,16} *In vivo*, a role for α A-crystallin in lens development and/or maintenance is supported by gene knockout studies in mice demonstrating progressive cataract formation relative to wild type.^{17–19} Furthermore, missense mutations in the α -crystallins have been implicated in congenital cataract.^{20–22} More recently, a similar role of α -crystallin in the development and transparency of the zebrafish lens was demonstrated.²³

Extensive *in vitro* experimentation has characterized the chaperone function of α -crystallin with a number of model and endogenous substrates, revealing common principles of activity in the sHSP superfamily. α -Crystallin has been found to delay aggregation of thermally²⁴ or chemically²⁵ denatured targets. More importantly and similar to other sHSP, α -crystallin binds destabilized proteins without the onset of gross aggregation. Using T4 lysozyme (T4L) as a client protein, we demonstrated that sHSP binding involves two modes distinguished by the

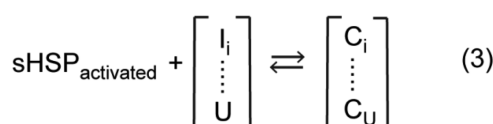
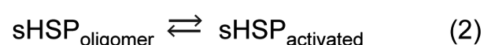
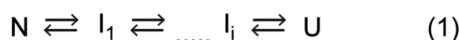
Received: June 17, 2015

Revised: August 24, 2015

Published: September 17, 2015

number of binding sites and affinity.^{26–30} Furthermore, sHSP affinity correlates with the degree of thermodynamic perturbation of the substrate,²⁷ establishing the sHSPs as “stability sensors”. Substrate binding can be increased under conditions that mimic environmental stress, such as changes in temperature,³¹ oxidation,³² or phosphorylation state^{26,33} of the chaperone (Scheme 1).

Scheme 1. Thermodynamic Model of sHSP Function^a



^aEquation 1 describes the equilibrium transition of a substrate between the native (N) and unfolded (U) states, including a continuum of non-native intermediates (I). Equation 2 states the equilibrium between the inactive oligomeric form of the sHSP and the activated, binding-competent species. Formation of a sHSP/substrate complex (“C” in Equation 3) depends on the population of activated sHSP and the recognized non-native states of the substrate.

A salient feature of sHSPs is the ability to form oligomeric assemblies of varying order.³⁴ α A- and α B-crystallin protomers associate into large polydisperse homo- and hetero-oligomers that approach 0.8 MDa on average. In general, the broad, dynamic range of oligomer size, symmetry, and order for sHSPs appears to be encoded by the primary sequence. Invariably, the oligomeric building block consists of a dimer assembled from the α -crystallin domain,^{35–37} 80–100 residues that form a beta-sandwich structure. This conserved motif is nestled between the variable N- and C-terminal domains.⁷ Crystallographic studies have shown that plasticity in oligomeric architecture is conferred by structural elements in the N-terminal domain and the C-terminal extension.^{38–40}

Importantly, a growing body of evidence implicates oligomer dynamics in sHSP activation.^{41–43} For instance, structural and functional studies of Hsp16.5 and Hsp27 have revealed two distinct mechanisms of chaperone function in which the N-terminus plays a critical role in oligomer assembly and substrate binding. Equilibrium dissociation from the native oligomer to a binding-competent dimer was inferred from studies of high affinity binding by Hsp27.^{30,44} In contrast, crystallographic and functional studies of the symmetric Hsp16.5 uncovered oligomer expansion facilitated by the plasticity of packing of the N-terminal domain and the dynamic properties of the C-terminal tail.^{40,45} These disparate mechanisms are unified by a central theme of increased accessibility to substrate binding sites in the N-terminal domain that are otherwise sequestered within the confines of the oligomer. Collectively, the hallmark of the high affinity binding mode is defined by global unfolding of the target substrate and sequestration into the core of the sHSP oligomer.^{33,46}

These observations suggest that sequence variation can shape the landscape of sHSP oligomer dynamics and, consequently, chaperone properties as defined by binding affinity and capacity. In this context, sequence divergence and the presence of species-specific chaperones may represent the blueprint of

evolutionary strategies to tune chaperone function. For instance, zebrafish is the first vertebrate discovered to express two different α B paralogous chains, α Ba and α Bb, yet displays striking sequence divergence⁴⁷ (Figure S1 of the [Supporting Information](#)). Interestingly, α Bb is more similar to human α B (58% identity) than to its paralog α Ba (50% identity). Whereas α Ba expression is limited to the lens in adults, α Bb mimics the ubiquitous extra-lenticular expression pattern of human α B, which suggests varying physiological roles. In rodent families, the species-specific α -crystallin α A^{ins} arises from alternative splicing of the primary α A-crystallin gene transcript that introduces a 23-amino acid polypeptide between residues E63 and L64 prior to the conserved α -crystallin domain.⁴⁸

Mechanistic knowledge encoded in this protein evolution process remains untapped. Therefore, we initiated a systematic investigation of the relationship between sequence divergence, oligomeric assembly, and chaperone activity in species-specific α -crystallins. Here, we compare the *in vitro* chaperone activity of the zebrafish α -crystallins with rat α A^{ins} and human chaperones. Combining equilibrium binding experiments and multiangle light scattering (MALS), we show that these α -crystallins display unique global oligomeric profiles that correlate to distinct chaperone activities. Furthermore, rat α A^{ins} and lens-specific zebrafish α Ba demonstrate intrinsically elevated binding activity toward destabilized T4L, which is reminiscent of fully activated mammalian sHSPs. These results support a conserved role for α -crystallin as a chaperone in the vertebrate lens, yet emphasizes structural and functional differences as a consequence of sequence variation within a species.

EXPERIMENTAL PROCEDURES

Materials. Monobromobimane was purchased from Toronto Research Chemicals Inc. Zebrafish α -crystallins were generous gifts from Dr. Mason Posner, Ashland University.

Mutagenesis. T4L mutants were generated by the QuikChange procedure (Stratagene) using complementary oligonucleotide primers containing the desired mutation and amplified via PCR. Construct integrity was confirmed by DNA sequencing.

Expression and Purification of Crystallins. The α -crystallin and Hsp27 constructs were expressed in *Escherichia coli* BL21/DE3 cells at 32 °C for 3 h after induction at mid-Log phase by 400 mM isopropyl β -D-thiogalactopyranoside (IPTG). Zebrafish α A, rat α A^{ins}, human α A or α B, the triply phosphorylated analogue (S19D/S45D/S59D) of α B-crystallin (referred to as α B-D3), and the triply phosphorylated analogue (S15D/S78D/S82D) of Hsp27 (referred to as Hsp27-D3) were purified as previously described.^{26,30,49} Protein concentrations for zebrafish α A, rat α A^{ins}, human α A, α B or α B-D3, and Hsp27-D3 were determined from extinction coefficients: 17 427, 19 940, 16 507, 19 005, and 40 529 M^{−1} cm^{−1}, respectively.

Zebrafish α Ba and α Bb were purified by anion exchange chromatography followed by size exclusion chromatography (SEC). Briefly, the cell pellets were lysed in Buffer A (20 mM Tris pH 8, 1 mM EDTA, 0.02% (w/v) sodium azide), and the homogenate was cleared by centrifugation after precipitation of chromatin by polyethylenimine. The proteins were eluted from HiTrap Q-column by linear sodium chloride gradient. Zebrafish α Ba-L was further purified by reverse phase chromatography. The samples eluted from the anion exchange column were adjusted to contain 0.5 M ammonium sulfate and then loaded

onto a phenyl-Sepharose column. Protein was eluted by a gradient from 0.5 to 0 M ammonium sulfate. All proteins were purified finally by SEC on Superose6 column into SEC buffer composed of 9 mM MOPS/6 mM Tris pH 7.2, 50 mM sodium chloride, 0.1 mM EDTA, 0.02% (w/v) sodium azide. Predicted molar extinction coefficients of 26 935 and 8479 M⁻¹ cm⁻¹ were used to determine α Ba and α Bb concentrations, respectively.

Expression and Purification of T4L. T4L mutants were expressed in *E. coli* BL21/DE3 cells and purified by sequential cation exchange and SEC as previously described.^{27,50} Following elution from the cation exchange column, the mutants were incubated with a 10-fold molar excess of monobromobimane for 2 h at room temperature and then overnight at 4 °C to label the Cys at residue 151. The protein was purified from unbound label by SEC using a Superdex75 column equilibrated with SEC buffer. The protein concentrations were determined using an extinction coefficient of 22 879 M⁻¹ cm⁻¹ for T4L mutants.

Molar Mass Determination. Molar mass of α -crystallins were determined by the multiangle laser light-scattering detector (Wyatt Technologies) connected in-tandem to a refractive index detector (Agilent). 100 μ L of each protein at 0.25–1 mg mL⁻¹ concentrations was injected by an Agilent HP1100 HPLC system on a Superose6 column equilibrated in the SEC buffer at the isocratic flow rate of 0.5 mL min⁻¹. The elution of the proteins was also monitored by a UV absorbance detector. The molar mass of the proteins were calculated by Astra software (Wyatt).

Equilibrium Binding Assay. Indicated concentrations (3 or 5 μ M) of T4L mutants were mixed with the chaperones at the stated molar ratio in SEC buffer, and the mixtures were incubated at defined temperatures for 2 h. Bimane fluorescence was measured in SynergyH4 microplate reader (BioTek) maintained at 37 °C. The bimane label was excited at 380 nm (band-pass 20 nm), and the fluorescence intensities parallel (I_{\parallel}) and perpendicular (I_{\perp}) to the direction of polarized light were recorded at 460 nm (band-pass 40 nm). These intensities were used to determine the steady state anisotropy (r) by the following equation: $r = (I_{\parallel} - I_{\perp}) / (I_{\parallel} + 2I_{\perp})$. Binding isotherms were generated by plotting bimane anisotropy as a function of the [sHSP]/[T4L] ratio. Each curve represents the average of two independent measurements. Curves were fit using the Levenberg-Marquart nonlinear least-squares method in the program Origin (OriginLab Inc.).³³ and proceeded with floating initial parameters. The maximum anisotropy was restricted to 0.4, and n (capacity) was bounded between 0.2 and 1.25. In some cases, reduced χ^2 of the fits was further improved by fixing n to the previously converged value. The resulting parameters are reported in tables with the standard deviation (s.d.) of the fit.

RESULTS

Methodology. Since previous work has revealed a correlation between oligomer dynamics of sHSP and chaperone activity,⁴³ we combined MALS experiments to define the global oligomeric properties of molar mass and polydispersity (defined as the range of molecular weights sampled across the main elution peak) with *in vitro* equilibrium binding experiments to determine the affinity and capacity of zebrafish α -crystallins and rat α A^{ins} to destabilized T4L. The substrate binding assay exploits the coupled equilibria described in Scheme 1. In this minimalist model, conditions which drive the substrate folding

equilibrium toward non-native/unfolded states (eq 1) or increase the activated population of the sHSP (eq 2) will enhance substrate association with the chaperone (eq 3).

To promote substrate recognition and binding by α -crystallins, we used a panel of previously characterized background mutations²⁷ in T4L that reduce the free energy of unfolding (ΔG_{unf}) relative to wild type as shown in Table 1.

Table 1. Stability Profile of T4L Mutants

T4L construct	ΔG_{unf} (kcal mol ⁻¹) ^a		
	23 °C (\pm s.d.)	30 °C (\pm s.d.)	37 °C (\pm s.d.)
WT	14.3 (1.5)		
D70N	9.2 (0.6)	7.8 (0.7)	6.8 (0.4)
L99A	7.9 (0.7)	6.5 (0.3)	5.3 (0.7)
L99A/A130S	6.6 (0.5)	4.7 (0.3)	3.5 (0.3)

^aDetermined at pH 7.2.

T4L mutants were labeled with a bimane fluorophore at a unique Cys in the C-terminal domain (T151 Bi) previously shown not to affect ΔG_{unf} .³³ These mutants possess equilibrium folding constants on the order of 10²–10⁴ at 37 °C, and crystallographic analysis indicates that such mutants retain native folds regardless of thermodynamic destabilization.⁵¹ Under conditions of the binding assay, the equilibrium of bimane-labeled T4L mutants predominately favors the folded state. Thus, the measured binding activity of the α -crystallins is coupled directly to the substrate folding equilibrium (eq 1 of Scheme 1). We have previously shown that binding interactions with T4L capture the intrinsic properties of sHSPs, which govern chaperone activity toward endogenous substrates.^{52,53}

Complex formation was monitored by changes in bimane anisotropy, which has been shown to be an effective reporter of α -crystallin/T4L binding.⁵⁴ Titration of α -crystallin restricts probe rotation leading to an increase in anisotropy, and the resulting binding isotherms yield properties, such as affinity, that distinguish chaperone activity between sHSPs. We opted to use anisotropy as the detection scheme for binding to enable the use of a high-throughput plate reader for data collection. Absent from anisotropy curves is the biphasic binding isotherms typically obtained from monitoring changes in bimane emission intensity, which is the signature of two-mode binding.²⁹ A monotonic increase in bimane anisotropy implies similar anisotropy values for both binding modes, precluding thorough parametrization of the second low affinity mode by nonlinear least-squares analysis. Therefore, anisotropy experiments were performed with low T4L concentrations to reduce the contribution of low affinity binding, and binding isotherms were fit with a single-site binding model to quantify binding sites (n) and affinity (K_D). In some experiments, values of n greater than 0.25 implied a minor role of the second binding mode,^{27,29} thus the reported K_D also represents a convolution of high and low affinity binding in these cases.

Oligomeric Diversity of Zebrafish α -Crystallins and Rat α A^{ins}. Recombinant zebrafish α A, α Ba, α Bb, and rat α A^{ins} were expressed and isolated using established protocols (Experimental Procedures) for biophysical characterization by MALS. Zebrafish α Ba displayed an unusual chromatographic behavior in the ion exchange step. The protein eluted at two different ionic strengths suggestive of two distinct protein populations with different global surface electrostatics. One population, hereafter referred to as α Ba-S, bound the resin and purified under similar conditions as zebrafish α A and α Bb. The

other population, referred to α Ba-L, was not retained by the resin at pH 8.0–8.5 and constituted approximately 35% of the total recoverable protein. Subsequent size exclusion chromatography revealed distinct elution patterns in which the α Ba-S peak was delayed by ~ 5.5 mL relative to α Ba-L (Figure 1).

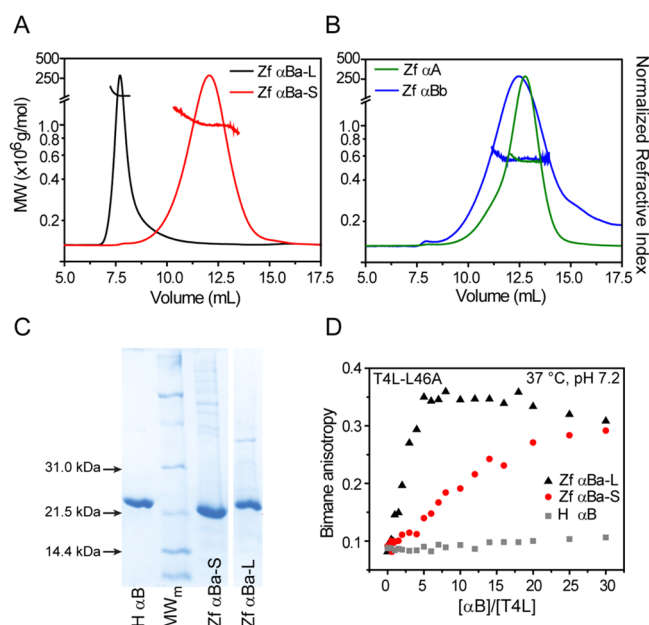


Figure 1. Oligomeric properties of zebrafish α -crystallins. (A) Purification of α Ba isolated two populations with distinct chromatographic behaviors and MALS profiles, revealing average molecular weights greater than 1×10^6 g mol⁻¹. (B) In contrast, α A and α Bb formed smaller oligomers of similar mass as reported in Table 2. (C) SDS-PAGE confirmed that α Ba and α Bb oligomers were constructed from subunit monomers of comparable molecular weight and purity. (D) Titration of a constant concentration of bimane-labeled T4L (3 μ M for α Ba-L and α Ba-S, 5 μ M for human α B) with α -crystallin increases bimane anisotropy, indicative of complex formation. Parallel to the differences in oligomer size, α Ba-L demonstrated elevated binding activity to the T4L-L46A substrate relative to α Ba-S. In contrast, very little binding of this T4L mutant by human α B was detected.

MALS analysis indicated that the molar mass of α Ba-L was substantially larger than α Ba-S, although both were polydisperse relative to α A and α Bb (Figure 1A,B). Importantly, α Ba-S and α Ba-L oligomers were built by the same monomeric unit as corroborated by comparable size and purity on SDS-PAGE (Figure 1C), and LC-MS/MS spectrometry following tryptic digestion (data not shown). The isolated α Ba-L population was stable and not influenced by concentration or pH (data not shown), suggesting that the two populations of α Ba are meta-equilibrium forms of the oligomer.

Remarkably, α Ba-S and α Ba-L demonstrated distinct chaperone activities according to anisotropy binding curves to the bimane-labeled T4L-L46A mutant ($\Delta G_{\text{unf}} = 6.6 \pm 0.4$ kcal mol⁻¹ at 37 °C³³). The apparent left shift in the α Ba-L titration implied a substantial enhancement of substrate binding relative to α Ba-S (Figure 1D). Combined, these results suggested that α Ba-S and α Ba-L, although derived from the same primary sequence, can segregate into two forms with very different oligomeric structures and chaperone activities.

We focused on α Ba-S since this population demonstrated comparable binding and oligomeric properties to other

zebrafish and rodent α -crystallins (Figure 1, Figure S2). Relative to α Ba-S, zebrafish α A and α Bb formed smaller oligomers that clustered around a similar average molar mass (Figure 1B, Table 2). The calculated molar mass of rat αA^{ins}

Table 2. Global Oligomer Properties Determined from MALS

α -crystallin	avg molar mass ($\times 10^6$ g/mol)	calculated no. of subunits ^a
human α A	0.773	36
rat αA^{ins}	0.447	20
zebrafish α A	0.556	28
zebrafish α Ba-S	1.035	48
zebrafish α Ba-L	$\gg 1.0$	$\gg 48$
zebrafish α Bb	0.587	32

^aDetermined by dividing the average molar mass by the monomer molecular weight.

was reduced approximately 50% on average (~ 0.4 MDa) in comparison to human α A, which is a consequence of increased polydispersity (Figure S2, Table 2). Indeed, MALS analysis indicated that αA^{ins} assembled into oligomers with a 0.9–0.2 MDa molecular weight range.

Zebrafish α -Crystallins and Rat αA^{ins} Are Protein Stability Sensors with a Spectrum of Affinities to Substrates. The propensity of zebrafish α -crystallins and αA^{ins} to form a complex with T4L mutants is illustrated by anisotropy binding curves at 37 °C and compared with human α A (Figures 2 and 3). Consistent with previous studies, a leftward shift in the binding curves of human α A between distinct T4L mutants indicated a change in capacity (n), affinity (K_D) or both. These changes are correlated with substrate ΔG_{unf} (Figure 2a, Table 3). A similar trend in binding pattern emerged from zebrafish α A and rat αA^{ins} (Figure 2b,c) and zebrafish α B crystallins (Figure 3) in which the most destabilized T4L-L99A/A130S mutant was bound with the highest efficiency. Invariably, T4L-L99A/A130S induced an increase in n relative to more stable mutants, suggesting an unavoidable contribution of the second low affinity-high capacity binding mode (Table 3). Analysis of binding curves generated from α -crystallin-induced quenching of bimane fluorescence intensity yielded similar changes in n and K_D (data not shown).

In accordance with the differences in global oligomeric properties (Figure 1), we observed species-specific changes in chaperone activity between α -crystallins. Collectively, the data sets in Figures 2 and 3 reported substantial variation in binding to T4L substrates. Interestingly, zebrafish α Ba-S, α Bb, and rat αA^{ins} demonstrated equivalent or greater tendency for complex formation with all T4L substrates relative to human and zebrafish α A. Whereas fits to the binding isotherms of all α A-crystallins to T4L-D70N were underdetermined due to limited binding, fits for α Ba-S, α Bb and αA^{ins} were better defined showing that the mutant bound with greater affinities (Table 3). Notably, binding curves with L99A and L99A/A130S were essentially indistinguishable for αA^{ins} (Figure 2c) and α Ba-S (Figure 3a), suggesting that these chaperones possess a higher intrinsic activity than human α A and zebrafish α A or α Bb.

Overall, these results are consistent with previous reports of related α -crystallins functioning as “stability sensors” in which the extent of binding depends on the substrate ΔG_{unf} (eq 1 of Scheme 1). Furthermore, the observed differences in chaperone

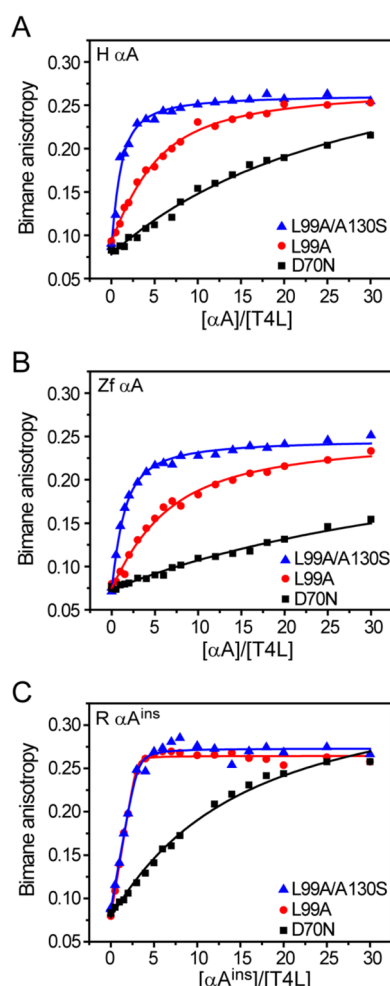


Figure 2. Binding profiles of α A-crystallins to destabilized T4L mutants. An increase in α -crystallin binding affinity and/or capacity is observed with a progressive decrease in T4L stability, which is reported as a left-shift in the data. Whereas the binding pattern of human (A) and zebrafish (B) α A are comparable, rat α A^{ins} (C) shows substantial enhancement of activity. Solid lines are the nonlinear least-squares fits of the curves and the parameters are reported in Table 3. All binding curves were generated in pH 7.2 buffer at 37 °C.

activity between orthologs and paralogs correlated with molecular weight and/or polydispersity of the sHSP oligomer (Figure 1). The average molar mass, polydispersity and binding of zebrafish α B-crystallins exceeded the α A chain. Likewise, enhanced binding activity of α A^{ins} relative to α A was consonant with the altered structural properties of the oligomer. Thus, these observations are in agreement with coupling between oligomer size, polydispersity and chaperone function.

Temperature Dependence of Chaperone Activity.

Previous reports have suggested that zebrafish α -crystallins, particularly α B-crystallins, display optimized chaperone activities at temperatures that approximate the physiological temperature of zebrafish (~28 °C).^{47,55} These studies, based on the suppression of aggregation of chemically denatured target substrates by the chaperone, indicated that zebrafish α -crystallin activity decreases at elevated temperatures (above 35 °C), which was contrasted with human α -crystallins that displayed higher chaperone-like activity at higher temperatures. These results were interpreted to imply that temperature dependence of chaperone function is an evolutionarily tuned

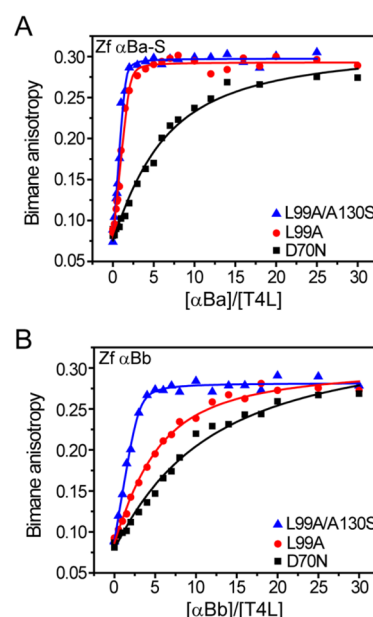


Figure 3. Zebrafish α B-crystallins demonstrate distinct binding behavior. Similar to α A, the α B paralogs showed increased binding activity toward more destabilized substrates. However, α Ba-S (A) binds the T4L mutants with higher affinity and capacity than α Bb (B). Binding isotherms were generated in pH 7.2 buffer at 37 °C, and the resulting fit parameters are shown in Table 3.

Table 3. Capacity and Affinity of α -Crystallins for T4L Mutants

α -crystallin	T4L	[T4L] μ M	N (\pm s.d.)	K_D (\pm s.d.) μ M
human α A	D70N	3	0.20 ^a	14.65 (3.21)
	L99A		0.27 (0.09)	2.43 (1.42)
	L99A/130S		1.25 ^a	2.37 (0.31)
rat α A ^{ins}	D70N	3	0.20 ^a	6.82 (1.03)
	L99A		0.33 (0.01)	0.017 (0.017)
	L99A/130S		0.32 (0.03)	0.064 (0.059)
zebrafish α A	D70N	5	0.20 ^a	88.92 (31.04)
	L99A		0.33 ^a	8.16 (1.07)
	L99A/130S		1.25 ^a	6.20 (0.44)
zebrafish α Ba-S	D70N	3	0.20 ^a	1.87 (0.31)
	L99A		0.47 (0.04)	0.058 (0.057)
	L99A/130S		0.65 (0.05)	0.063 (0.060)
zebrafish α Bb	D70N	3	0.20 ^a	4.85 (0.87)
	L99A		0.20 (0.04)	1.34 (0.17)
	L99A/130S		0.33 (0.02)	0.12 (0.06)

^an was fixed during the fitting routine. See Experimental Procedures.

feature adapted for the native environment of the organism.⁴⁷ We explored this hypothesis further in binding assays by exploiting the temperature dependence of ΔG_{unf} of different T4L substrates (Table 1) to uncover temperature-induced changes in zebrafish α -crystallin chaperone activity.

In contrast to previous reports, a general trend emerged from the binding isotherms of zebrafish α -crystallins in which changes in n and K_D reflected greater binding affinity and capacity with increasing temperature from 28 to 37 °C as illustrated in Figure 4 for α A and α Bb. In addition, lowering the temperature from 28 to 23 °C decreased the binding affinity of α Bb at least 5-fold. This pattern of temperature-dependent binding was independent of substrate ΔG_{unf} as shown in Table

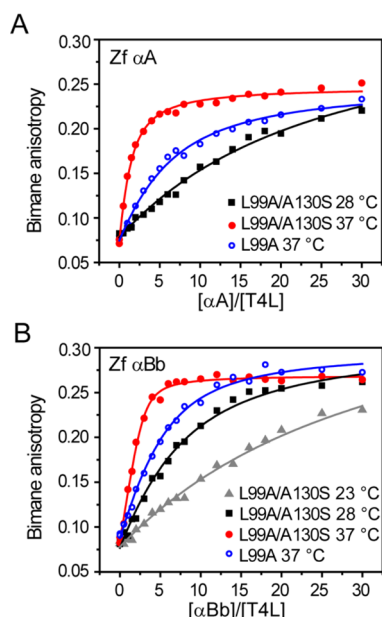


Figure 4. Temperature-driven activation of zebrafish α -crystallin chaperone activity. A left-shift in the binding curves is induced by an increase in temperature for α A (A) and α Bb (B). Specific activation of the α -crystallins can be seen by comparing substrate binding of T4L-L99A at 37 °C and -L99A/A130S at 28 °C. At these temperatures, both substrates possess similar ΔG_{unf} , which implies the increased binding affinity is a consequence of enhanced chaperone activity. The parameters for the fits are reported in Table 4.

4. Moreover, zebrafish α A showed the lowest affinity toward T4L in all conditions, yet α Ba-S consistently demonstrated the greatest binding activity.

Changes in temperature shift the folding constant of the T4L substrates by 2 orders of magnitude across the tested temperature range (Table 1). Thus, the observed activation of chaperone binding at higher temperatures is driven partially by a shift in the substrate folding equilibrium toward non-native

Table 4. Temperature Dependence of Zebrafish α -Crystallin Binding Activity

α -crystallin	T4L	[T4L] μM	temp (°C)	N (\pm s.d.)	K_D (\pm s.d.) μM
α A	L99A	5	28	0.20 ^a	50.71 (12.69)
	L99A	5	37	0.33 ^a	8.16 (1.07)
	L99A/ 130S	5	28	0.20 ^a	20.87 (3.82)
	L99A/ 130S	5	37	1.25 ^a	6.20 (0.44)
α Ba-S	L99A	5	28	0.20 (0.04)	0.92 (0.71)
	L99A	3	37	0.64 (0.05)	0.012 (0.034)
	L99A/ 130S	5	28	0.28 (0.02)	0.21 (0.12)
	L99A/ 130S	3	37	0.65 (0.05)	0.063 (0.060)
α Bb	L99A	3	37	0.20 (0.04)	1.34 (0.17)
	L99A/ 130S	5	23	0.20 ^a	28.96 (5.87)
	L99A/ 130S	5	28	0.20 ^a	4.94 (0.76)
	L99A/ 130S	3	37	0.34 (0.02)	0.25 (0.08)

^a n was fixed during the fitting routine. See Experimental Procedures

states (eq 1). However, a parallel temperature-dependent shift in the α -crystallin oligomer equilibrium toward a larger pool of binding competent species (eq 2) will also contribute to the apparent increase in chaperone activity (eq 3). Therefore, in order to deconvolute temperature-driven changes of eq 2, we compared binding isotherms of T4L-L99A at 37 °C with T4L-L99A/130S at 28 °C. On the basis of the stability profiles (Table 1), these T4L mutants are expected to have near identical ΔG_{unf} at the respective temperatures, and thus similar equilibrium folding constants. In the context of Scheme 1, this approach masks the role of eq 1 while ascribing differences in binding curves to temperature-driven activation of the α -crystallins to promote substrate association. As shown in Figure 4, binding of T4L-L99A at 37 °C was enhanced relative to T4L-L99A/A130S at 28 °C for both zebrafish α A and α Bb with an increase in binding affinity approximately three- to 10-fold (Table 4). A similar increase in capacity and affinity was observed for α Ba-S for these substrates, reinforcing the conclusion that increasing temperature, even beyond 28 °C, activates binding by the chaperone in stark contrast with the conclusions of Dahlman and colleagues⁵⁵ (Table 4).

Zebrafish α Ba and Rodent α A^{ins} Are Activated Chaperones. Although zebrafish and rat α -crystallins displayed properties as predicted by the thermodynamic model of chaperone function, a direct comparison of binding revealed strong functional divergence (Figure 5). Whereas zebrafish and human α A bind T4L-L99A with relatively similar affinities, the K_D of rat α A^{ins} was more than 100-fold lower than zebrafish or human α A (Figure 5a, Table 5). Differences in binding activity were even more pronounced for the α B-crystallins. The zebrafish paralogs showed substantially elevated binding with respect to human α B (Figure 5b). However, variations in activity within the zebrafish α B chains were also apparent in which α Ba-S bound the destabilized substrate with an order of magnitude higher affinity and with greater capacity than α Bb (Table 5). As a group, zebrafish α B-crystallins demonstrated greater binding activity than zebrafish α A. Both of these observations disagree with previously reported results.^{47,55}

Remarkably, the binding affinity of α Ba-S and α A^{ins} is similar to that of the phosphorylation mimics (D3 analogues, Experimental Procedures) of mammalian sHSPs. As shown in Figure 5c, these α -crystallins bind T4L-L99A with a similar efficiency as fully activated human α B-D3 and Hsp27-D3. The binding parameters reported in Table 5 likewise underscore relatively minor differences n and K_D for these chaperones. This result suggests that these species-specific chaperones have evolved particularly to provide a steady-state buffering capacity against protein aggregation.

DISCUSSION

The results presented above offer a novel perspective on the evolutionary tuning of α -crystallin chaperone activity. In addition to establishing the roles of rodent α A^{ins} and zebrafish α -crystallins as chaperones, our observations highlight distinct structural and functional features that arise from sequence divergence within paralogs. The general properties of rodent α A^{ins} and zebrafish α -crystallins *in vitro* chaperone activity are described well by the thermodynamic model of Scheme 1. Substrates with progressive reductions in ΔG_{unf} trigger higher affinity binding by the chaperone, indicating that these α -crystallins can discriminate between target proteins on the basis of the equilibrium population of non-native states. Similar to other species and sHSPs, zebrafish α -crystallin displays

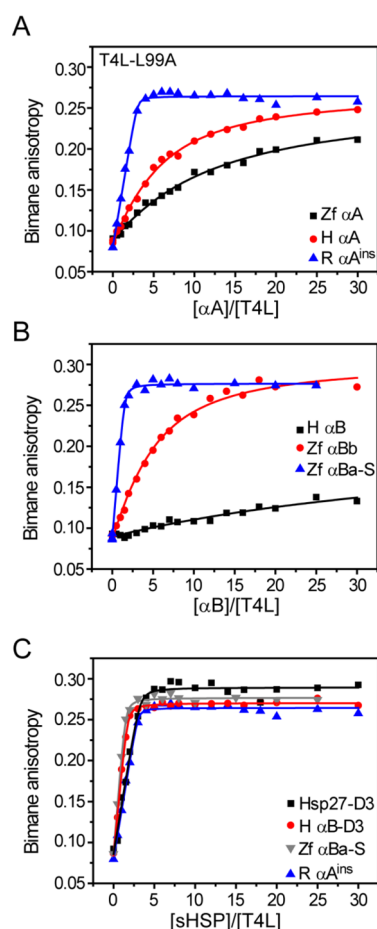


Figure 5. Species-specific activation of α -crystallin binding activity. Binding to T4L-L99A is compared to each species expressing orthologs of α A (A), α B (B) and activated chaperones (C). Zebrafish α Ba-S and rat α A^{ins} show similar binding patterns as fully activated sHSPs. Fit parameters are reported in Table 5. All binding curves were generated in pH 7.2 buffer at 37 °C with a [T4L] of 3 μ M.

Table 5. Comparison of sHSP Binding to T4L-L99A between Species

sHSP	N (\pm s.d.)	K_D (\pm s.d.)
human α A	0.21 (0.05)	1.90 (0.95)
human α B	0.20 ^a	27.95 (17.08)
human α B-D3	0.58 (0.02)	0.071 (0.026)
human Hsp27-D3	0.30 (0.02)	0.038 (0.041)
rat α A ^{ins}	0.33 (0.01)	0.017 (0.017)
zebrafish α A	0.27 ^a	8.32 (0.95)
zebrafish α Ba-S	0.65 (0.03)	0.068 (0.035)
zebrafish α Bb	0.20 (0.04)	1.34 (0.71)

^an was fixed during the fitting routine. See Experimental Procedures.

temperature-driven activation, even above the hypothesized threshold of 28 °C. These results imply that the energetic component of chaperone function in sHSPs is governed by common principles across the evolutionary spectrum.

However, definitive differences in substrate binding among the α -crystallins investigated here uncovered functional characteristics which deviate from previously reported results. Although α A and α Ba are lens-specific in adult zebrafish, α Ba was described as having reduced chaperone-like activity relative to α A, α Bb, and human α B in assays which measured

suppression of target protein aggregation under denaturing conditions.^{47,55} This led to the hypothesis that α Ba has little utility as a chaperone in the lens. The binding assay performed here, which quantitatively describes the predominant molecular interactions that precede aggregation, illustrates that α Ba possesses larger capacity and greater affinity toward destabilized substrates than α A and α Bb as defined by larger n and a smaller K_D .

A similar observation was evident for rat α A^{ins} relative to α A in our binding experiments. In contrast, results from earlier studies have presented the appearance of α A^{ins} in the rodent genome as an evolutionary conundrum. The ability of α A^{ins} to prevent aggregation of target proteins in nonequilibrium assays was reduced compared to α A, conferring no apparent advantage as a chaperone to overall lens maintenance.⁵⁶ This result led to the unsatisfying speculation that α A^{ins} has been selectively retained as a structural protein in the lens, even though it contributes only 10–20% of the total α A-crystallin pool⁴⁸ and has been lost in most mammalian species.⁵⁷ We find that rat α A^{ins} is more active as a chaperone than α A, binding the identical substrate up to 2 orders of magnitude higher affinity.

A major finding of this work is that α A^{ins} and α Ba-S bind substrates at levels that approach other fully activated sHSPs. As shown in Figure 5, α A^{ins} and α Ba-S produce comparable binding isotherms with the phosphorylation-mimic D3 analogues of human α B and Hsp27. This remarkable result suggests that zebrafish α Ba-S and rat α A^{ins} encode for chaperones that operate in a highly activated state in the absence of regulatory control.

Importantly, we emphasize that α Ba-S and α A^{ins} binding characteristics are representative of *intrinsic* function since the observed activity was achieved without protein modification, such as phosphorylation. Phosphorylated forms of zebrafish^{58,59} and rodent α A-crystallins⁶⁰ have been found to increase with age and can be stimulated by chemical stress,⁶¹ which suggests the potential to modulate chaperone activity. Zebrafish α Ba and α Bb contain only one and two of the three consensus phosphorylation sites found in human α B,⁶² respectively (Figure S1). Currently, no phosphorylation of α B-crystallins has been found in zebrafish.⁵⁸ In light of results presented here, significant variations in the primary sequence of zebrafish α Ba may have resulted in the loss of a phosphorylation “switch” and contributed to the generation of a chaperone with constitutively enhanced activity.

Other sequence elements have been shown to influence oligomer properties with a concomitant change in chaperone activity. The N-terminus of Hsp27 and Hsp16.5 mediates oligomer dissociation^{30,63} or expansion,⁴⁵ respectively, to activate high affinity binding. In this study, the most active species displayed the potential to form large (α Ba) and/or polydisperse (α A^{ins}) oligomers with a broad range of incorporated subunits. The most likely source of increased polydispersity in α A^{ins} is the spliced peptide located in the N-terminal domain. Interestingly, the location of this insertion is reminiscent of a critical peptide in Hsp27 that is important for oligomer dynamics and binding.⁴⁴ Potentiated substrate binding exhibited by α A^{ins} likewise suggests a correlation between enhanced oligomer dynamics and chaperone function relative to α A. Sequence divergence within the N- and C-terminal domains of zebrafish α B-crystallins (Figure S1) appear to support distinct oligomeric and functional properties. Indeed the formation of higher order oligomers of α Ba (i.e., α Ba-L)

with even greater chaperone activity than α Ba-S may be related to unique subunit packing arrangements (Figure 1).

The differences in α -crystallin chaperone activity, even between paralogs, presumably reflects the requirement for the tissue in which it is expressed. In the context of an avascular lens devoid of *de novo* protein synthesis, age-related exhaustion of soluble, intact α -crystallin ushers protein aggregation and may contribute to initiation of cataractogenesis.^{60,64,65} An intriguing observation is that zebrafish and rat α -crystallins are far less represented in total lens protein relative to humans although the ratio of α A to α B is similar.^{58,66} This difference in crystallin profile has been interpreted as a reflection of animal lifespan, or as a consequence of greater γ -crystallin content. However, the presence of a permanently activated α -crystallin in zebrafish (α Ba) and rat (α A^{ins}) lenses would be advantageous as a mechanism to compensate for the overall reduced α -crystallin pool.

A number of studies have established parallels between mammalian and zebrafish α -crystallins that support the use of zebrafish as a model system for vertebrate lens proteostasis.^{23,58,59,67} *In vitro* characterization of the chaperone function supports a conserved role for α -crystallin in lens maintenance. Additionally, expression of duplicate genes with divergent sequence and function offers a unique opportunity to investigate the evolutionary approach toward sHSP design within a species. Indeed, the results presented here provide a framework to interpret subsequent mutagenesis studies designed to interrogate sequence variation between zebrafish α -crystallins.

■ ASSOCIATED CONTENT

■ Supporting Information

The Supporting Information is available free of charge on the ACS Publications website at DOI: 10.1021/acs.biochem.5b00678.

Sequence alignments of α -crystallins and MALS analysis of rat α A^{ins} (PDF)

■ AUTHOR INFORMATION

Corresponding Author

*Address: Department of Molecular Physiology and Biophysics 741 Light Hall, 2215 Garland Ave, Nashville, TN 37232. Telephone: (615) 322-3307. E-mail: hassane.mchaourab@vanderbilt.edu.

Author Contributions

[‡]H.A.K. and D.P.C. contributed equally. H.A.K. designed, performed experiments, and analyzed data with the help of S.M. and E.T.M. D.P.C. performed data analysis and wrote the manuscript. R.A.S. performed MALS of α A^{ins}. H.S.M. contributed to all aspects.

Funding

This work was supported by a National Institutes of Health Grant R01 EY12018 to H.S.M.

Notes

The authors declare no competing financial interest.

■ DEDICATION

This work is dedicated to the memory of Dr. Hanane A. Koteiche.

■ ABBREVIATIONS

sHSP, small heat shock protein chaperone; T4L, T4 lysozyme; MALS, multiangle light scattering; SEC, size exclusion chromatography

■ REFERENCES

- (1) Piatigorsky, J. (1981) Lens differentiation in vertebrates. A review of cellular and molecular features. *Differentiation* 19, 134–153.
- (2) Bloemendal, H., de Jong, W., Jaenicke, R., Lubsen, N. H., Slingsby, C., and Tardieu, A. (2004) Ageing and vision: structure, stability and function of lens crystallins. *Prog. Biophys. Mol. Biol.* 86, 407–485.
- (3) Delaye, M., and Tardieu, A. (1983) Short-range order of Crystallin proteins accounts for eye lens transparency. *Nature* 302, 415–417.
- (4) Tardieu, A. (1988) Eye lens proteins and transparency: from light transmission theory to solution X-ray structural analysis. *Annu. Rev. Biophys. Biomol. Struct.* 17, 47–70.
- (5) Jaenicke, R. (1994) Eye-lens proteins: structure, superstructure, stability, genetics. *Naturwissenschaften* 81, 423–429.
- (6) Ingolia, T. D., and Craig, E. A. (1982) Four small Drosophila heat shock proteins are related to each other and to mammalian alpha-Crystallin. *Proc. Natl. Acad. Sci. U. S. A.* 79, 2360–2364.
- (7) de Jong, W. W., Caspers, G. J., and Leunissen, J. A. (1998) Genealogy of the α -Crystallin–small heat-shock protein superfamily. *Int. J. Biol. Macromol.* 22, 151–162.
- (8) Horwitz, J. (1992) α -Crystallin can function as a molecular chaperone. *Proc. Natl. Acad. Sci. U. S. A.* 89, 10449–10453.
- (9) Hanson, S. R., Hasan, A., Smith, D. L., and Smith, J. B. (2000) The major *in vivo* modifications of the human water-insoluble lens crystallins are disulfide bonds, deamidation, methionine oxidation and backbone cleavage. *Exp. Eye Res.* 71, 195–207.
- (10) Lampi, K. J., Amyx, K. K., Ahmann, P., and Steel, E. A. (2006) Deamidation in human lens betaB2-Crystallin destabilizes the dimer. *Biochemistry* 45, 3146–3153.
- (11) Nagaraj, R. H., Linetsky, M., and Stitt, A. W. (2012) The pathogenic role of Maillard reaction in the aging eye. *Amino Acids* 42, 1205–1220.
- (12) Santhoshkumar, P., Raju, M., and Sharma, K. K. (2011) alphaA-Crystallin peptide SDRDKFVIFLDVKHF accumulating in aging lens impairs the function of alpha-Crystallin and induces lens protein aggregation. *PLoS One* 6, e19291.
- (13) van den Berg, B., Ellis, R. J., and Dobson, C. M. (1999) Effects of macromolecular crowding on protein folding and aggregation. *EMBO J.* 18, 6927–6933.
- (14) van den Berg, B., Wain, R., Dobson, C. M., and Ellis, R. J. (2000) Macromolecular crowding perturbs protein refolding kinetics: implications for folding inside the cell. *EMBO J.* 19, 3870–3875.
- (15) Horwitz, J. (1993) Proctor Lecture. The function of α -Crystallin. *Invest. Ophthalmol. Visual Sci.* 34, 10–22.
- (16) Benedek, G. B. (1997) Cataract as a protein condensation disease: the Proctor Lecture. *Invest. Ophthalmol. Visual Sci.* 38, 1911–1921.
- (17) Andley, U. P., Malone, J. P., Hamilton, P. D., Ravi, N., and Townsend, R. R. (2013) Comparative proteomic analysis identifies age-dependent increases in the abundance of specific proteins after deletion of the small heat shock proteins alphaA- and alphaB-Crystallin. *Biochemistry* 52, 2933–2948.
- (18) Boyle, D. L., Takemoto, L., Brady, J. P., and Wawrousek, E. F. (2003) Morphological characterization of the Alpha A- and Alpha B-Crystallin double knockout mouse lens. *BMC Ophthalmol.* 3, 3.
- (19) Brady, J. P., Garland, D., Duglas-Tabor, Y., Robison, W. G., Jr., Groome, A., and Wawrousek, E. F. (1997) Targeted disruption of the mouse aA-Crystallin gene induces cataract and cytoplasmic inclusion bodies containing the small heat shock protein aB-Crystallin. *Proc. Natl. Acad. Sci. U. S. A.* 94, 884–889.
- (20) Litt, M., Kramer, P., LaMorticella, D. M., Murphey, W., Lovrien, E. W., and Weleber, R. G. (1998) Autosomal dominant congenital

cataract associated with a missense mutation in the human α -Crystallin gene CRYAA. *Hum. Mol. Genet.* 7, 471–474.

(21) Mackay, D., Andley, U., and Shiels, A. (2003) Cell death triggered by a novel mutation in the α -Crystallin gene underlies autosomal dominant cataract linked to chromosome 21q. *Eur. J. Hum. Genet.* 11, 784–793.

(22) Vicart, P., Caron, A., Guicheney, P., Li, Z., Prevost, M. C., Faure, A., Chateau, D., Chapon, F., Tome, F., Dupret, J. M., Paulin, D., and Fardeau, M. (1998) A missense mutation in the α B-Crystallin chaperone gene causes a desmin-related myopathy. *Nat. Genet.* 20, 92–95.

(23) Zou, P., Wu, S. Y., Koteiche, H. A., Mishra, S., Levic, D. S., Knapik, E., Chen, W., and McHaourab, H. S. (2015) A conserved role of α -Crystallin with spin-labeled peptides in the development of the zebrafish embryonic lens. *Exp. Eye Res.* 138, 104–113.

(24) Jakob, U., Gaestel, M., Engel, K., and Buchner, J. (1993) Small heat shock proteins are molecular chaperones. *J. Biol. Chem.* 268, 1517–1520.

(25) Farahbakhsh, Z. T., Huang, Q. L., Ding, L. L., Altenbach, C., Steinhoff, H. J., Horwitz, J., and Hubbell, W. L. (1995) Interaction of α -Crystallin with spin-labeled peptides. *Biochemistry* 34, 509–516.

(26) Koteiche, H. A., and McHaourab, H. S. (2003) Mechanism of chaperone function in small heat-shock proteins. Phosphorylation-induced activation of two-mode binding in α B-Crystallin. *J. Biol. Chem.* 278, 10361–10367.

(27) McHaourab, H. S., Dodson, E. K., and Koteiche, H. A. (2002) Mechanism of Chaperone Function in Small Heat-Shock Proteins. Two-Mode Binding of the Excited States of T4 Lysozyme Mutants by α A-Crystallin. *J. Biol. Chem.* 277, 40557–40566.

(28) Sathish, H. A., Koteiche, H. A., and McHaourab, H. S. (2004) Binding of destabilized β B2-Crystallin mutants to α -Crystallin: the role of a folding intermediate. *J. Biol. Chem.* 279, 16425–16432.

(29) Sathish, H. A., Stein, R. A., Yang, G., and McHaourab, H. S. (2003) Mechanism of chaperone function in small heat-shock proteins. Fluorescence studies of the conformations of T4 lysozyme bound to α B-Crystallin. *J. Biol. Chem.* 278, 44214–44221.

(30) Shashidharamurthy, R., Koteiche, H. A., Dong, J., and McHaourab, H. S. (2005) Mechanism of chaperone function in small heat shock proteins: dissociation of the HSP27 oligomer is required for recognition and binding of destabilized T4 lysozyme. *J. Biol. Chem.* 280, 5281–5289.

(31) Reddy, G. B., Das, K. P., Petrash, J. M., and Surewicz, W. K. (2000) Temperature-dependent chaperone activity and structural properties of human α A- and α B-crystallins. *J. Biol. Chem.* 275, 4565–4570.

(32) Wang, K., and Spector, A. (1995) α -Crystallin can act as a chaperone under conditions of oxidative stress. *Invest. Ophthalmol. Visual Sci.* 36, 311–321.

(33) Claxton, D. P., Zou, P., and McHaourab, H. S. (2008) Structure and orientation of T4 lysozyme bound to the small heat shock protein α A-Crystallin. *J. Mol. Biol.* 375, 1026–1039.

(34) Haley, D. A., Bova, M. P., Huang, Q. L., McHaourab, H. S., and Stewart, P. L. (2000) Small heat-shock protein structures reveal a continuum from symmetric to variable assemblies. *J. Mol. Biol.* 298, 261–272.

(35) Koteiche, H. A., and McHaourab, H. S. (1999) Folding pattern of the α -Crystallin domain in α A-Crystallin determined by site-directed spin labeling. *J. Mol. Biol.* 294, 561–577.

(36) Bagneris, C., Bateman, O. A., Naylor, C. E., Cronin, N., Boelens, W. C., Keep, N. H., and Slingsby, C. (2009) Crystal Structures of α -Crystallin Domain Dimers of α B-Crystallin and Hsp20. *J. Mol. Biol.* 392, 1242–1252.

(37) Jehle, S., Rajagopal, P., Bardiaux, B., Markovic, S., Kuhne, R., Stout, J. R., Higman, V. A., Klevit, R. E., van Rossum, B. J., and Oschkinat, H. (2010) Solid-state NMR and SAXS studies provide a structural basis for the activation of α B-Crystallin oligomers. *Nat. Struct. Mol. Biol.* 17, 1037–1042.

(38) Laganowsky, A., Benesch, J. L. P., Landau, M., Ding, L., Sawaya, M. R., Cascio, D., Huang, Q., Robinson, C. V., Horwitz, J., and

Eisenberg, D. (2010) Crystal structures of truncated α A and α B crystallins reveal structural mechanisms of polydispersity important for eye lens function. *Protein Sci.* 19, 1031–1043.

(39) Laganowsky, A., and Eisenberg, D. (2010) Non-3D domain swapped crystal structure of truncated zebrafish α A Crystallin. *Protein Sci.* 19, 1978–1984.

(40) McHaourab, H. S., Lin, Y., and Spiller, B. W. (2012) Crystal structure of an activated variant of small heat shock protein Hsp16.5. *Biochemistry* 51, 5105–5112.

(41) Basha, E., O'Neill, H., and Vierling, E. (2012) Small heat shock proteins and α -crystallins: dynamic proteins with flexible functions. *Trends Biochem. Sci.* 37, 106–117.

(42) Jehle, S., Vollmar, B. S., Bardiaux, B., Dove, K. K., Rajagopal, P., Gonen, T., Oschkinat, H., and Klevit, R. E. (2011) N-terminal domain of α B-Crystallin provides a conformational switch for multimerization and structural heterogeneity. *Proc. Natl. Acad. Sci. U. S. A.* 108, 6409–6414.

(43) McHaourab, H. S., Godar, J. A., and Stewart, P. L. (2009) Structure and mechanism of protein stability sensors: chaperone activity of small heat shock proteins. *Biochemistry* 48, 3828–3837.

(44) McDonald, E. T., Bortolus, M., Koteiche, H. A., and McHaourab, H. S. (2012) Sequence, structure, and dynamic determinants of Hsp27 (HspB1) equilibrium dissociation are encoded by the N-terminal domain. *Biochemistry* 51, 1257–1268.

(45) Shi, J., Koteiche, H. A., McHaourab, H. S., and Stewart, P. L. (2006) Cryoelectron Microscopy and EPR Analysis of Engineered Symmetric and Polydisperse Hsp16.5 Assemblies Reveals Determinants of Polydispersity and Substrate Binding. *J. Biol. Chem.* 281, 40420–40428.

(46) Shi, J., Koteiche, H. A., McDonald, E. T., Fox, T. L., Stewart, P. L., and McHaourab, H. S. (2013) Cryoelectron microscopy analysis of small heat shock protein 16.5 (Hsp16.5) complexes with T4 lysozyme reveals the structural basis of multimode binding. *J. Biol. Chem.* 288, 4819–4830.

(47) Smith, A. A., Wyatt, K., Vacha, J., Vihtelic, T. S., Zigler, J. S., Jr., Wistow, G. J., and Posner, M. (2006) Gene duplication and separation of functions in α B-Crystallin from zebrafish (*Danio rerio*). *FEBS J.* 273, 481–490.

(48) King, C. R., and Piatigorsky, J. (1984) Alternative splicing of α A-Crystallin RNA. Structural and quantitative analyses of the mRNAs for the α A2- and α A1s-Crystallin polypeptides. *J. Biol. Chem.* 259, 1822–1826.

(49) Berengian, A. R., Bova, M. P., and McHaourab, H. S. (1997) Structure and function of the conserved domain in α A-Crystallin. Site-directed spin labeling identifies a β -strand located near a subunit interface. *Biochemistry* 36, 9951–9957.

(50) McHaourab, H. S., Lietzow, M. A., Hideg, K., and Hubbell, W. L. (1996) Motion of spin-labeled side chains in T4 lysozyme. Correlation with protein structure and dynamics. *Biochemistry* 35, 7692–7704.

(51) Eriksson, A. E., Baase, W. A., and Matthews, B. W. (1993) Similar hydrophobic replacements of Leu99 and Phe153 within the core of T4 lysozyme have different structural and thermodynamic consequences. *J. Mol. Biol.* 229, 747–769.

(52) McHaourab, H. S., Kumar, M. S., and Koteiche, H. A. (2007) Specificity of α A-Crystallin binding to destabilized mutants of β B1-Crystallin. *FEBS Lett.* 581, 1939–1943.

(53) Mishra, S., Stein, R. A., and McHaourab, H. S. (2012) Cataract-linked γ D-Crystallin mutants have weak affinity to lens chaperones α -crystallins. *FEBS Lett.* 586, 330–336.

(54) Koteiche, H. A., and McHaourab, H. S. (2006) Mechanism of a Hereditary Cataract Phenotype: Mutations in α A-Crystallin activate substrate binding. *J. Biol. Chem.* 281, 14273–14279.

(55) Dahlman, J. M., Margot, K. L., Ding, L., Horwitz, J., and Posner, M. (2005) Zebrafish α -crystallins: protein structure and chaperone-like activity compared to their mammalian orthologs. *Mol. Vis.* 11, 88–96.

(56) Smulders, R. H., van Geel, I. G., Gerards, W. L., Bloemendal, H., and de Jong, W. W. (1995) Reduced chaperone-like activity of α

A(ins)-Crystallin, an alternative splicing product containing a large insert peptide. *J. Biol. Chem.* 270, 13916–13924.

(57) Hendriks, W., Sanders, J., de Leij, L., Ramaekers, F., Bloemendal, H., and de Jong, W. W. (1988) Monoclonal antibodies reveal evolutionary conservation of alternative splicing of the alpha A-Crystallin primary transcript. *Eur. J. Biochem.* 174, 133–137.

(58) Posner, M., Hawke, M., Lacava, C., Prince, C. J., Bellanco, N. R., and Corbin, R. W. (2008) A proteome map of the zebrafish (*Danio rerio*) lens reveals similarities between zebrafish and mammalian Crystallin expression. *Mol. Vis.* 14, 806–814.

(59) Wages, P., Horwitz, J., Ding, L., Corbin, R. W., and Posner, M. (2013) Changes in zebrafish (*Danio rerio*) lens Crystallin content during development. *Mol. Vis.* 19, 408–417.

(60) Ueda, Y., Duncan, M. K., and David, L. L. (2002) Lens proteomics: the accumulation of Crystallin modifications in the mouse lens with age. *Invest. Ophthalmol. Visual Sci.* 43, 205–215.

(61) Wang, K., Gawinowicz, M. A., and Spector, A. (2000) The effect of stress on the pattern of phosphorylation of aA and aB Crystallin in the rat lens. *Exp. Eye Res.* 71, 385–393.

(62) Miesbauer, L. R., Zhou, X., Yang, Z., Sun, Y., Smith, D. L., and Smith, J. B. (1994) Post-translational modifications of water-soluble human lens crystallins from young adults. *J. Biol. Chem.* 269, 12494–12502.

(63) Lambert, H., Charette, S. J., Bernier, A. F., Guimond, A., and Landry, J. (1999) HSP27 multimerization mediated by phosphorylation-sensitive intermolecular interactions at the amino terminus. *J. Biol. Chem.* 274, 9378–9385.

(64) Grey, A. C., and Schey, K. L. (2009) Age-related changes in the spatial distribution of human lens alpha-Crystallin products by MALDI imaging mass spectrometry. *Invest. Ophthalmol. Visual Sci.* 50, 4319–4329.

(65) Stella, D. R., Floyd, K. A., Grey, A. C., Renfrow, M. B., Schey, K. L., and Barnes, S. (2010) Tissue localization and solubilities of alphaA-Crystallin and its numerous C-terminal truncation products in pre- and postcataractous ICR/f rat lenses. *Invest. Ophthalmol. Visual Sci.* 51, 5153–5161.

(66) Lampi, K. J., Shih, M., Ueda, Y., Shearer, T. R., and David, L. L. (2002) Lens proteomics: analysis of rat Crystallin sequences and two-dimensional electrophoresis map. *Invest. Ophthalmol. Visual Sci.* 43, 216–224.

(67) Goishi, K., Shimizu, A., Najarro, G., Watanabe, S., Rogers, R., Zon, L. I., and Klagsbrun, M. (2006) AlphaA-Crystallin expression prevents gamma-Crystallin insolubility and cataract formation in the zebrafish cloche mutant lens. *Development* 133, 2585–2593.